WAT's Up with using the Small Angle Approximation to Estimate Climb Gradient Limited Departure Weights

Timothy T. Takahashi[1]
Philip R. Thomas[2]

Arizona State University, Tempe, AZ

This paper expands upon problems that arise when engineers use the classic work-energy-theorem equation, climb gradient equals thrust minus drag over weight, to predict climb performance. These equations are commonly used to schedule the WAT limit; the maximum allowable takeoff weight that guarantees a minimum climb capability in the event of an engine failure. The classic formulation relies upon a small-angle-approximation form of the work-energy-theorem. In this new work, we examine the continuing implications of using the full equations of motion to determine the schedule performance. An increase in predicted allowable payload is permissible if the engineer considers the implications of the general equations of motion.

I. Introduction

MODERN COMMERICAL AIRCRAFT are safe and reliable means of transport precisely because they are designed and operated in a manner that reduces risks associated with foreseeable failures. [1][2][3][4] For example, commercial aircraft are not allowed to dispatch unless their runway performance is sufficient to suffer an engine failure at most inopportune time and either safely brake to a stop (without the use of reverse thrust) or continue to flight within the limits of the departure runway. [5][6][7][8] Regulations require dispatch to consider sufficient reserve performance in the event of engine failure to overfly obstacles [9]; in previous papers, my students and I have written on this topic. [10][11][12] In this work, we discuss how the minimum regulatory limit for engine-operative climb performance can potentially limit the dispatch weight. [13]

This paper seeks to clarify the implications of the commonly used small-angle-approximation work-energy theorem when used to determine this limit.

II. Background

It is important to understand the distinction between the field-performance limited takeoff weight, the climb-gradient limited takeoff weight and the obstacle clearance limited takeoff weight. Safe and legal dispatch must not allow an aircraft to depart unless its combined load renders its takeoff weight to be at or less than most restrictive of these three values. [8]

Unlike the field-performance limited takeoff weight (which is a general function of weather as well as runway geometry) or the obstacle-clearance limited takeoff weight (which is a general function of weather as well as the terrain surrounding an airport), the climb-gradient limited takeoff weight is an intrinsic function of the aircraft itself. The climb-gradient is a straightforward function of aerodynamic characteristics, weight, engine performance, airfield pressure altitude and outside temperature. Consequently, the climb-gradient limited takeoff weight is often called the **WAT Limit** (Weight / Altitude / Temperature).

[1] Professor of Practice, Aerospace and Mechanical Engineering, School for Engineering of Matter, Transport & Energy, P.O. Box 876106, Tempe, AZ, 85287. Associate Fellow AIAA.

[2] M.S. Candidate, Aerospace and Mechanical Engineering, School for Engineering of Matter, Transport & Energy, P.O. Box 876106, Tempe, AZ, 85287. Member AIAA

A. Multi-Segment Takeoff Process

To reiterate, the FAA defines the takeoff procedure as broken into several phases and segments.[14][15]

The entirety of takeoff can be divided into two phases: the ground phase (when the airplane is physically rolling on the runway) and the air phase (when the aircraft is airborne, even it is still above the runway).

The air phase may be broken into five or six segments.

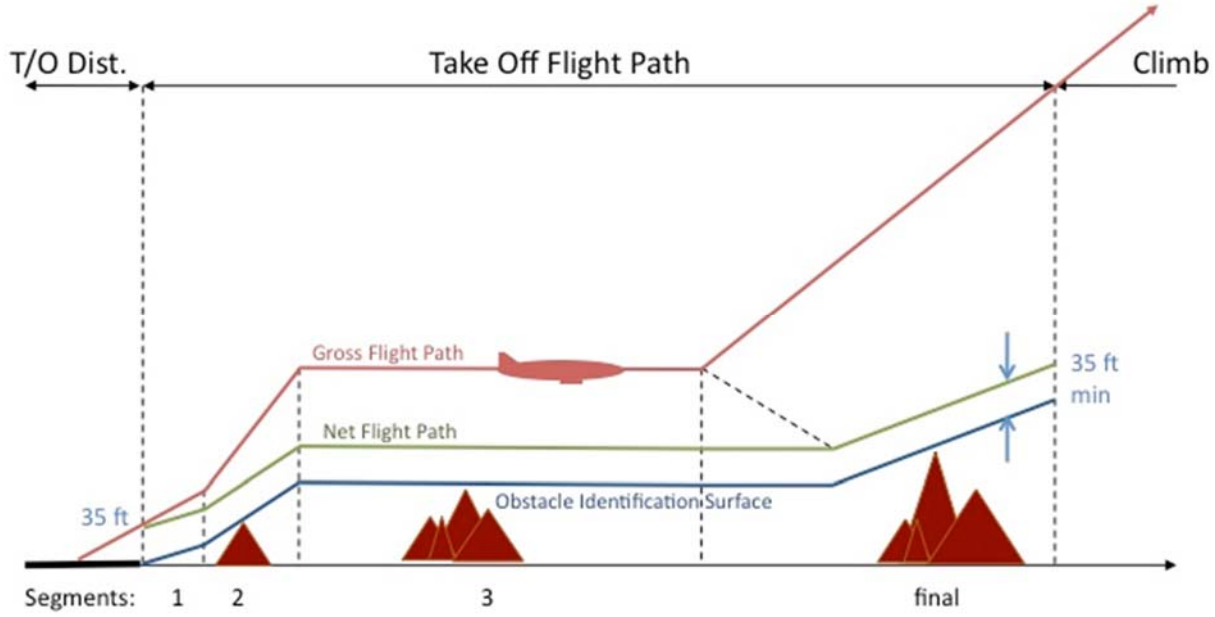

FIGURE 1 – Multi-Segment Takeoff Procedure

The initial air phase, before the aircraft reaches an altitude of 35-ft above the runway surface is considered as part of the transition to flight. Flight begins just as the aircraft wheels leave the runway, but the aircraft is unsettled and pilot control inputs are required to stabilize the flight at a constant indicated airspeed. [13] The ground distance covered during these early moments of flight are bookkept with the ground phase distance as part of published the critical field length distance. [7]

The first segment [13] begins as the aircraft passes 35-ft above-ground-level, and the pilot initiates landing gear retraction. Because the gear and gear doors cycle during this segment, the aerodynamic drag may change markedly. The thrust during first segment climb reflects the takeoff thrust setting with speed dependent lapse effects fully accounted for. In the event of an engine failure, an automatic thrust control system (ATTCS) [16][17] may alter the thrust level of the remain engines. Engineers schedule the takeoff rotation speed (*VR*) so that under engine-inoperative conditions the aircraft will attain the second-segment climb speed, *V2*, as the aircraft passes 35-ft above-ground level. [18] Under normal conditions, the speed throughout this segment is not constant; the aircraft will accelerate through the *V2* speed.

The second segment [13] begins at the point that the landing gear is fully retracted and pilot achieves a stable climb. Second segment ends with flap retraction; under normal circumstances, the minimum flap retraction altitude is 400-ft above the runway elevation. Pilots fly second segment climb with flaps at the takeoff departure setting holding indicated (or calibrated) airspeed (KIAS or KCAS) constant. Thus, pilots maintain essentially constant aerodynamic coefficients (*CL* and *CD*) during second segment climb. Pilots hold the thrust settings on the operating engines at their initial takeoff setting. Because of changes in airspeed and elevator (static pressure and temperature effects) the thrust will lapse somewhat as the aircraft climbs. Under engine inoperative conditions, pilots are trained to fly second segment climb at the published *V2* speed. Under normal conditions, pilots stabilize climb at whatever airspeed the aircraft attains after gear retraction (typically *V2*+10 or even *V2*+15 knots). Because second segment climb is flown

at constant KIAS, the true airspeed KTAS of the aircraft increases slightly as the aircraft gains altitude and the air density decreases. The ground speed of the aircraft is greatly impacted by the presence of headwinds or tailwinds. Since winds shift and the thrust and true airspeed change as the aircraft climbs, the second segment climb gradient is not a constant. Regulations require engineers to publish and guarantee second-segment climb gradient predictions to be accurate or pessimistic up to an altitude 400-ft above the airfield. [13]

For dispatch planning, third segment is a level flight segment where the aircraft converts all of its surplus energy into kinetic as opposed to potential energy. Here, the aircraft will accelerate from its second-segment climb speed to the minimum flap retraction speed, *VFR*. The pilot will then initiate flap retraction. This segment ends when flaps have retracted and the aircraft has attained its fourth segment climb speed, *V4* or *Vfuss*. [19] The thrust levels of all operating engines remain at their takeoff setting. The level acceleration procedure is used only in the even of an engine failure. In a normal takeoff, pilots will continue to climb (albeit more leisurely) and accelerate to flap retraction speed by slightly depressing the nose. After flap retraction, pilots will reduce the engine power levers from takeoff setting to an enroute climb setting (often designated Maximum Climb Thrust or Maximum Continuous Thrust).

The fourth, or final climb segment, is a flaps up climb flown at constant IAS and maximum continuous thrust. It continues until the aircraft has overflown all significant terrain or exceeds 1500-ft above-ground-level. Since winds shift and the thrust and true airspeed change as the aircraft climbs, the fourth segment climb gradient is not constant. Regulations require engineers to publish and guarantee fourth-segment climb gradient predictions to be accurate or pessimistic up to an altitude 1,500-ft above the airfield. [15]

B. Regulatory Minimums

The FAA (and EASA) publish very specific regulations that limit the aircraft dispatch weight to ensure minimum engine-inoperative climb performance.

The key governing regulations are [15][18][13] summarized here:

14 CFR § 25.111 Takeoff path.
(a) The takeoff path extends from a standing start to a point in the takeoff at which the airplane is 1,500 feet above the takeoff surface, or at which the transition from the takeoff to the en route configuration is completed and *VFTO* is reached, whichever point is higher.

14 CFR § 25.107 Takeoff speeds.
(b)*V2*MIN, in terms of calibrated airspeed, may not be less than -
(1) 1.13 VSR for … Turbojet powered airplanes without provisions for obtaining a significant reduction in the one-engine-inoperative power-on stall speed; …
(3) 1.10 times VMC

(c)*V2*, in terms of calibrated airspeed, must be selected by the applicant to provide at least the gradient of climb required by § 25.121(b) but may not be less than … *V2*MIN

and

14 CFR § 25.121 Climb: One-engine-inoperative.

…

(b) Takeoff; landing gear retracted. In the takeoff configuration existing at the point of the flight path at which the landing gear is fully retracted, and in the configuration used in § 25.111 but without ground effect:
(1) The steady gradient of climb may not be less than 2.4 percent for two-engine airplanes, 2.7 percent for three-engine airplanes, and 3.0 percent for four-engine airplanes, at *V2* with:
(i) The critical engine inoperative, the remaining engines at the takeoff power or thrust available at … a height of 400 feet above the takeoff surface; and
(ii) The weight equal to the weight existing when the airplane's landing gear is fully retracted

…

(c) Final takeoff. In the en route configuration at the end of the takeoff path determined in accordance with § 25.111:
(1) The steady gradient of climb may not be less than 1.2 percent for two-engine airplanes, 1.5 percent for three-engine airplanes, and 1.7 percent for four-engine airplanes, at *VFTO* with -
(i) The critical engine inoperative and the remaining engines at the available maximum continuous power or thrust; and
(ii) The weight equal to the weight existing at the end of the takeoff path

…

(d) Approach. In a configuration corresponding to the normal all-engines-operating procedure in which VSR for this configuration does not exceed 110 percent of the VSR for the related all-engines-operating landing configuration:
(1) The steady gradient of climb may not be less than 2.1 percent for two-engine airplanes, 2.4 percent for three-engine airplanes, and 2.7 percent for four-engine airplanes, with -
(i) The critical engine inoperative, the remaining engines at the go-around power or thrust setting;
(ii) The maximum landing weight;
(iii) A climb speed established in connection with normal landing procedures, but not exceeding 1.4 VSR; and
(iv) Landing gear retracted.

EASA regulations CS 25.107 [21] CS 25.111 [22] and CS 25.121 [23] are essentially similar.

We engineers tend to consider that the amount of fuel burned during the takeoff ground phase and initial air phase is insignificant, so we will perform all dispatch climb calculations at the notional "takeoff weight."

The legacy of an early risk-based statistical model gives as a regulatory minimums which are funcitons of the flight phase (second and fourth segment) and the aircraft configuration (the number of engines).

Note that these climb-gradient limited weights needs to be guaranteed throughout the initial climb out (typically up to 400-ft above-ground-level for second-segment and 1,500-ft above-ground-level for fourth-segment).

Implicitly, the climb gradient requirements controlled by 14 CFR § 25.121 [13] are specified under nominal, zero-wind conditions. Consequently, compliance with these regulations guarantees a minimum level of kinematic performance but no particular ability to overfly any given obstacle. Obstacle clearance planning charts needed to demonstrate compliance with a standard instrument departure (SID) must take into account winds.

While the regulations talk about two distinct takeoff climb-gradient limit checks, we also must understand that the published WAT limit value represents the most restrictive of these cases. In many cases, the second segment climb limit weight is the lowest but in other cases the fourth segment climb limit weight may control. This duality prevents an easy algebraic solution of the problem, even assuming that thrust and drag could be modelled with simple algebraic formulae. In addition, many aircraft offer the pilot more than one takeoff flap setting – a less aggressive flap setting will often improve climb performance (and hence increase the WAT limit) at the expense of additional takeoff ground roll.

C. Classical Work Energy Theorem Approach

Recall that Newton's Second Law states: "the rate of change of momentum of a body is directly proportional to the force applied, and this change in momentum takes place in the direction of the applied force." [23] In other words, $\overrightarrow{\boldsymbol{F_{net}}} = \boldsymbol{m}\frac{\boldsymbol{d}}{\boldsymbol{dt}}\left(\vec{\boldsymbol{V}}\right) = \boldsymbol{m}\vec{\boldsymbol{a}}$**.** Similarly, in a frictionless environment (or its analogy, one with no net force imbalance), the sum of kinetic and gravitational potential energy must conserve: $\frac{\boldsymbol{1}}{\boldsymbol{2}}\,\boldsymbol{m}\,\boldsymbol{V^2} + \boldsymbol{mgh} = \boldsymbol{const}$**.** Thus, many aircraft performance texts apply these equations to estimate aircraft performance. [24][25][26][27]

The typical derivation makes many assumptions to attain the classic equation that the rate-of-climb expressed in ft/min is:

$$ROC = \frac{6080}{60} \cdot KTAS \cdot \frac{T-D}{W} = 101.3 \cdot KTAS \cdot \frac{T-D}{W} \quad (1)$$

where the velocity, *KTAS*, is in nM/hr, and thrust, *T*, drag, *D*, and weight, *W*, are all in equivalent units (pounds force (lbf) and pounds mass (lbm), or kilogram-force (kgf) / kilogram (kg)).

D. Boeing Short Course Approach

The Boeing Performance Short Course notes [28] mirror the classic derivation with one slight difference. They go beyond the unaccelerated rate-of-climb to hold forth a more general relationship. They introduce the ability to perform an "accelerated climb." Thus:

$$P_s = \frac{(T-D)\,V}{W} = \frac{dALT}{dt} \approx RoC_{unaccelerated} \quad (2)$$

where the actual rate-of-climb is best estimated as:

$$RoC = \frac{RoC_{unaccelerated}}{(1+\frac{VdV}{gdh})} \quad (3)$$

As before, this equation infers that the rate-of-climb is linearly proportional to P_s subject to a correction stemming from the fact that during takeoff pilots are expected to fly a constant indicated airspeed (*KIAS*) or calibrated airspeed (*KCAS*) trajectory.

As was noted before, during a climb at constant indicated airspeed, the aircraft must increase its kinetic energy as it ascends.

For this work, we presume that the compressibility corrections and other position errors are small, so we will conflate indicated, calibrated and equivalent airspeed: $EAS \cong CAS \cong IAS$.

Correction factors, based upon the standard atmosphere altitude lapse rate, can account for this effect. Thus, the small-angle approximation rate-of-climb at a given Mach number and altitude is:

$$ROC(M, ALT) \cong K_{accel} \cdot ROC_{\ unacelerated}(M, ALT) \quad (4)$$

Which, when applied to the structure of the 1962 and 1976 Standard Atmosphere model, results in:

$$K_{accel} = \frac{1}{1 + .566816 \cdot M^2} \quad (5)$$

for climb at constant equivalent airspeed at low altitudes.

E. Takahashi's Observations

The classic derivations (including those found in the Boeing Short Course) assume that:

- aerodynamic lift must equal weight, and
- the flight path angle may be represented by the work-energy-theorem derived function: *T/W – 1/(L/D)*

In Figure 2, we may examine the more generalized free-body-diagram. [29] Here, we can see that lift and drag are orthogonal to one another, thrust is aligned (and tracks with) the body axis of the aircraft which is rotated relative to the flight path by the aerodynamic angle of attack (α). Viewed in a horizon-level reference frame, the thrust acts at an angle ($\alpha+\gamma$) above the horizon. The reader should note that the flight path differs from the earth-horizon reference frame by the flight path angle (γ).

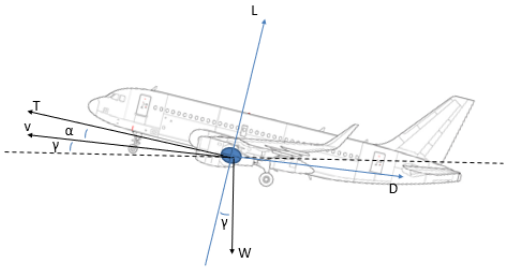

FIGURE 2 – Geometry - Aerodynamic Force Balance

While the cosine of moderate angles, for example $\alpha=10^o$, is nearly one, the sin is not that small: *sin (10º) ~ 0.17*. Thus, the thrust of an aircraft flying at angle of attack will materially offset its weight. This is a material difference which leads to differences between the classical equations and more complex simulations.

In AIAA 2015-2701, Takahashi noted that the Rutowski method for determining the optimum minimum-fuel-to-climb and minimum-time-to-climb flight trajectories when applied to high thrust-to-weight rocket planes and airliner configurations did not actually suggest an optimal trajectory. [30] In this paper, he concluded that "that the simplifications inherent in the work-energy theorem derived basic performance equations (flight at small angles of attack, thrust vector is aligned with drag, climb at small flight path angles (i.e. lift is aligned to oppose weight) … fundamentally detract from the veracity of the general method." [30]

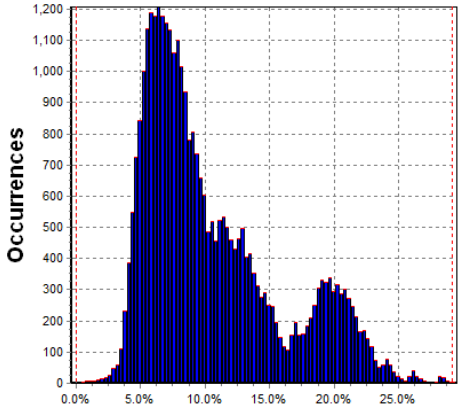

FIGURE 3 – Histogram of Exact vs. Work-Energy-Theorem Approximate Climb Gradient Prediction Differences (positive "error" means the actual gradient is better than the "work-energy-theorem" gradient – negative "error " means the actual gradient is worse than the "work-energy-theorem" gradient). (from AIAA 2019-1305 [32])

In AIAA 2018-0284, [31] Takahashi, Beard & Wood noted significant discrepancies when comparing the work-energy approach to flight performance against point-mass time step integrating simulation results. They found that work-energy was "not particularly accurate even for engine-inoperative climb at shallow gradients." [32] They postulate the following scenario:

> Consider an initial climbout with takeoff flaps: the aircraft may be pitched to 10º angle of attack although it flies at ~2.4% climb gradient (a 1.3º flight path angle), thus the aircraft attains a 11.3º deck angle. Because weight acts in the ground reference frame, the thrust from the remaining engines acts upon a vector displaced 11.3º from normal. Since lift and drag act in a reference frame aligned to the flight path angle, not to the aircraft body, a fraction of lift will offset weight. In the case of a notional A320 operating near its WAT limit, ~19.5% of the thrust (*sin(11.3º)*) offsets weight (~4,300-lbf lift relief from the 168,000-lbm flight weight) while 98% of the thrust (*cos(10º)*) opposes drag. This 2.5% relief in lift results in a ~5 .25% reduction in induced drag. The aircraft will climb better than predicted through work-energy because the ~5.25% induced drag reduction more than offsets the 2% loss in thrust. While these errors seem small, they compound. Their effects become evident when computing the climb profile of actual aircraft flown on typical missions particularly in fourth segment engine-inoperative climb.[31]

In AIAA 2019-1305 [32] Takahashi noted that this error can be quite significant. In a statistical study of 33,600 cases representing reasonable thrust, weight and aerodynamic properties of transport-category aircraft, he saw that the simplified work-energy-theorem climb gradient predicitons are often quite pessimistic. Turning to Figure 3, we see a histogram of the magnitude of the error. On this plot a positive "error" means the actual gradient is better than the work-energy-theorem gradient; the work-energy-theorem is pessimistic (and safe). Conversely, a negative "error" means the actual gradient is worse than the work-energy-theorem gradient; the work-energy-theorem is optimistic

(and unsafe). We see that the median error is ~8.8% pessimistic; but also note that mean error is considerably higher (~10.6% pessimistic). All analyzed cases are are safe. But the level of error observed, up to a 25%+ error in absolute gradient, is troublesome.

In this new work, we will examine consequences of the simplified work-energy-theorem climb gradient prediction as applied to the WAT limit.

III. Mathematical Basis for Modeling

This work begins following the fully generalized free-body-diagram that includes flight path angle (γ) and angle-of-attack (α); refer back to Figure 2. We well compare and contrast the rate-of-climb and climb-gradient predictions made for a variety of generic aircraft.

To begin, let us utilize the general equations of motion, this time expressed in an earth-horizon-fixed reference frame, and balanced for flight with no change in horizon level velocity and a constant rate-of-climb.

$$T\cos(\alpha+\gamma) - D\cos(\gamma) + L\,sin(\gamma) = 0 \tag{6A}$$

$$T\sin(\alpha+\gamma) - D\,sin(\gamma) + L\,cos(\gamma) = W \tag{6B}$$

Where dimensional lift and drag are represented as functions of coefficients as:

$$L = CL\;q\;Sref \tag{7A}$$

$$D = CD\;q\;Sref \tag{7B}$$

and

$$CL = \frac{dCL}{d\alpha}\alpha + CL_0 \tag{8}$$

Given this background, where the dynamic pressure, q, is governed by flight at the regulatory *V2* speed limit from 14 CFR § 25.107, we can numerically solve this pair of non-linear equations in two independent variables for both the angle of attack (α) and the flight path angle (γ). In this work, we use the internal gradient solver in EXCEL/VBA to converge the solution.

The climb gradients that we derive from the flight path angle (*GRAD = tan(γ)*) are functionally identical to those calculated using a time-step integrating point-mass-simulation set for zero acceleration.

We will compare this to the climb gradient based on the simple work-energy theorem

$$GRAD = \tan(\gamma) \approx \tan(\frac{T-D}{W}) \tag{9}$$

In addition to this comparison (where the aerodynamic efficiency *L/D* does not change as the weight is offset by thrust), we can also introduce a slight more complex aerodynamic model :

$$CD = CD_0 + \frac{CL^2}{\pi\,AR_{eff}} \tag{10}$$

In this formulation the lift coefficient is a dependent variable that is a function of lift, wing area and climb speed:

$$CL = \frac{L}{q\;Sref} = \frac{L}{\left(1481\left(\frac{KEAS}{660.8}\right)^2\right)Sref} \tag{11}$$

And subsequently, the dimensional drag (D) is also a dependent variable:

$$D = \left(CD_0 + \frac{CL^2}{\pi\, AR_{eff}}\right)(1481\ \left(\frac{KEAS}{660.8}\right)^2\ Sref) \qquad (12)$$

For engine inoperative climb, CD_0 will include the drag of basic airframe in takeoff configuration PLUS the windmill drag of the inoperative engine.

This paper will consider the effects of various aerodynamic, propulsive, mass-properties and human factors uncertainties upon the landing distances of a notional narrow-body twin-engine commercial airliner, reminiscent of an Airbus A320; thus, $Sref$ = 1319-ft^2. While the lift and drag models are simplified, they have been calibrated to provide reasonable quality quantitative and well as excellent qualitative predictive capabilities.

Transport category aircraft may have many different flap settings. At minimum, aircraft have three flap settings representing cruise, takeoff and landing. The Airbus A320, for example, has five settings: **UP**, **CONF 1+F, CONF 2, CONF 3** and **CONF FULL**. [33] Engineers design the aircraft so that the flaps up setting has ideal lift and drag divergence characteristics for en-route as well as high speed flight. **CONF 1+F** deploys the takeoff leading edge slats and minimally deploy the trailing edge flaps; this is one possible setting for takeoff. **CONF 2** further deploys the trailing flaps, increases the maximum lift coefficient (and reduces the stall speed); it is a typical takeoff setting for this aircraft. **CONF 3** extends the leading edge slats to a landing position and fully extends the trailing edge flaps; this provides a further increase in maximum lift coefficient but with some drag penalty. Finally, the **CONF FULL** flap setting offers maximally deflected the trailing edge flaps to provide the slowest stall speed possible, but with a further increase in drag.

The aerodynamic model used in this simulation was re-created from reverse-engineered A320 flight performance model developed by Beard [34] and utilized in previous works [10][11][12]. While attempting to match Airbus published climb performance, Beard derived zero-lift-drag increments appropriate for a variety of flap settings (**CONF 1+F**, **CONF 2**, **CONF 3** and **CONF FULL**), all-engines-operating and one-engine-inoperative flight with a windmilling engine, and flight with landing gear extended.

For this paper, we will restrict our analysis to second segment climb. That is, climb with the flaps in an initial takeoff setting (**CONF 2**) and the landing gear stowed.

Beard [34] reverse-engineered an aerodynamic model for multiple flap configurations; see Figure 4. The aerodynamic model accurately represents the increases in lift and drag for increasing flap extension. With the flaps set for takeoff at **CONF 2**, $CLmax$ is ~ 2.16. We can approximate the drag polar with CD_0 ~ 0.0450, AR_{eff} ~ 7.5 for **CONF 2** flaps (takeoff flaps). We believe that $dCL/d\alpha$ ~ 0.10/^{o} with flaps deployed. The zero lift angle of attack is α_0 ~ -3^o with flaps deployed. Beard also estimated that the drag increases due to an engine failing results in an increase in coefficient of drag of ΔCD ~ 0.0134. This aerodynamic model can closely replicated published A320 flight performance.

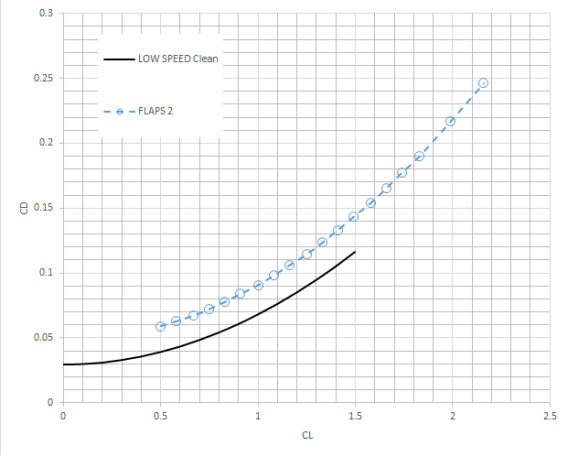

FIGURE 4 – Drag polars inferred from A320 published climb performance (gear up, AEO) [34]

For these analyses we use an NPSS model [35] to predict installed engine performance. We use this code to develop discrete tables (five-column data) representing

flight at standard and non-standard-day conditions (i.e. ISA+15ºC). Engine models may include maximum continuous thrust data as well as limited-duration (5-minute take-off or "go-around") enhanced power settings computed to higher turbine-inlet-temperatures.

We used NPSS to simulate the performance of a *BPR*=5.0 two-shaft turbofan engine with a 1.6:1 reference fan-pressure-ratio for the bypass flow and 33:1 reference overall-pressure-ratio for the core flow. Fuel flow limits keep the turbine inlet temperature at or below 2300ºF at maximum power. Thus, this model should exhibit the general characteristics of the IAE *V*2527-A6 turbofan engine as installed in many narrow-body Airbus airliners. [36] We run this model over a variety of flight speeds and altitudes with different ISA temperature deviations.

We may consider the effects of deviation in outside air temperature from the standard atmosphere. In Figure 5, we can see how the basic NPSS thermodynamic cycle model responds to changes in temperature. As the air becomes cooler than the reference temperature it gains in density. Because the engine can process more mass flow at the same volume flow rate and it can tolerate richer fuel-air mixtures within the same maximum turbine inlet temperature limit it will produce more thrust. Conversely, as the air becomes warmer than the reference temperature it loses density, requires leaner fuel-air mixtures and loses thrust. Under sea-level, static conditions, we see that roughly one-half of the thrust lapse with temperature is due to density-altitude effects and the other half is a function of practical turbine-inlet-temperature limits on fuel mixture.

Table 1 consists of a subset of five column data useful for takeoff performance analysis.

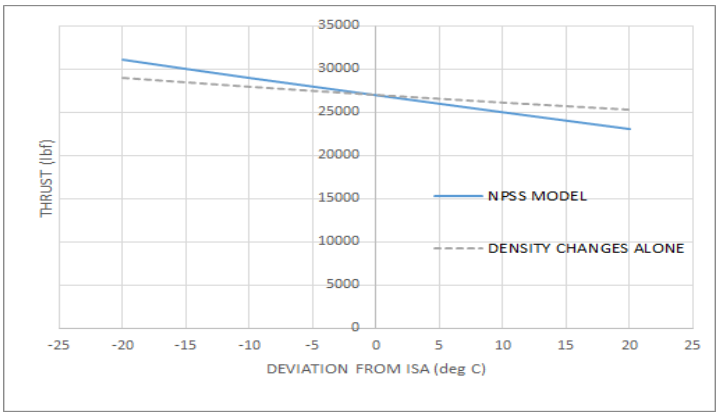

FIGURE 5 – NARROW BODY AIRCRAFT PROPULSION – Temperature Dependent Thrust Lapse at Sea Level Static Conditions

TABLE 1 - NARROW BODY AIRCRAFT AERODYNAMIC PROPULSION DATABASE reflecting a 27,000-lbf rated turbofan engine (ISA)

MACH	ALT	PLA	THRUST	TSFC
0	0	0.85	147.53	0.808
0	0	0.9	6989.49	0.319
0	0	0.96	14131.26	0.331
0	0	0.98	17045.64	0.344
0	0	1	27000	0.403
0	5000	0.85	7135.83	0.309
0	5000	0.9	7207.92	0.309
0	5000	0.96	13772.7	0.334
0	5000	0.98	16485.39	0.35
0	5000	1	23907.96	0.405
0	10000	0.85	3588.57	0.317
0	10000	0.9	7265.43	0.305
0	10000	0.96	13311.54	0.339
0	10000	0.98	14625.9	0.35
0	10000	1	15940.26	0.361
0.1	0	0.85	197.61	1.364
0.1	0	0.9	5719.14	0.388
0.1	0	0.96	12286.08	0.38
0.1	0	0.98	15022.26	0.39
0.1	0	1	24581.07	0.444
0.1	5000	0.85	5957.55	0.368
0.1	5000	0.9	6017.76	0.368
0.1	5000	0.96	12114.63	0.379
0.1	5000	0.98	14665.86	0.392
0.1	5000	1	21833.01	0.445
0.1	10000	0.85	2849.31	0.397
0.1	10000	0.9	6171.93	0.357
0.1	10000	0.96	11825.19	0.381
0.1	10000	0.98	13064.36	0.391
0.1	10000	1	14303.52	0.401
0.2	0	0.85	151.1	2.634
0.2	0	0.9	4713.93	0.463
0.2	0	0.96	10736.28	0.43
0.2	0	0.98	13307.22	0.436
0.2	0	1	22651.92	0.487
0.2	5000	0.85	744.12	0.963
0.2	5000	0.9	5058.45	0.432
0.2	5000	0.96	10715.22	0.425
0.2	5000	0.98	13085.82	0.436
0.2	5000	1	20174.94	0.487
0.2	10000	0.85	2285.55	0.487
0.2	10000	0.9	5275.53	0.413
0.2	10000	0.96	10539.45	0.424
0.2	10000	0.98	11684.79	0.4325
0.2	10000	1	12830.13	0.441
0.3	0	0.85	1205.01	0.923
0.3	0	0.9	3848.58	0.551
0.3	0	0.96	9405.99	0.483
0.3	0	0.98	11806.29	0.485
0.3	0	1	21113.73	0.53
0.3	5000	0.85	1535.49	0.72
0.3	5000	0.9	4232.79	0.503
0.3	5000	0.96	9475.65	0.473
0.3	5000	0.98	11684.79	0.481
0.3	5000	1	18854.64	0.529
0.3	10000	0.85	1795.23	0.602
0.3	10000	0.9	4506.57	0.473
0.3	10000	0.96	9401.13	0.469
0.3	10000	0.98	10470.2	0.4755

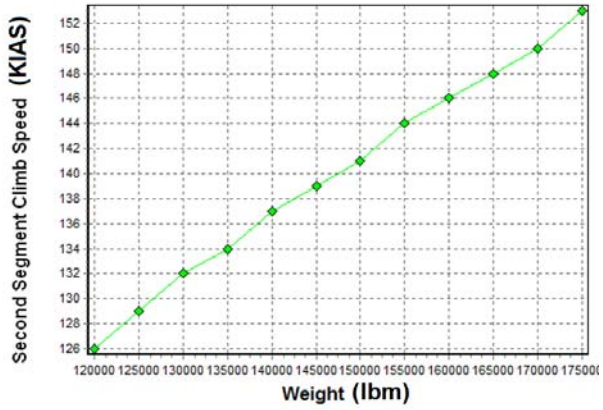

FIGURE 6: *V2* speed vs Weight (notional A320 model with CONF 2 flap setting, *CLmax* = 2.16, *V2*=1.13 *Vs* not limited by *VMCA*. Simulation ran at standard day sea-level conditions.

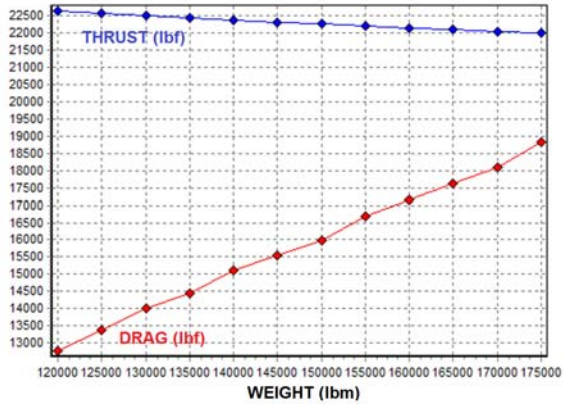

FIGURE 7: Dimensional thrust and drag as a function of takeoff Weight (notional A320 model with CONF 2 flap setting, *CLmax* = 2.16, *V2*=1.13*Vs* not limited by *VMCA*. Simulation ran at standard day sea-level conditions.

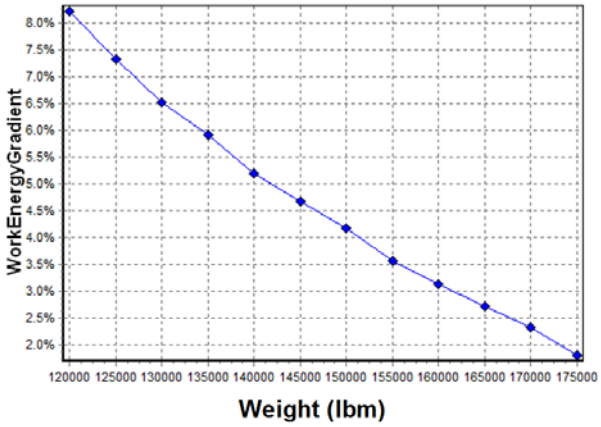

FIGURE 8: Simple thrust – drag over weight work-energy climb gradient prediction as a function of takeoff Weight (notional A320 model with CONF 2 flap setting, *CLmax* = 2.16, V2=1.13 Vs not limited by *VMCA*. Standard day sea-level conditions.

IV. Simulation Results

This section compares the predicted performance arising from the full equations of motion against that from the simplified, work-energy-theorem model. Ideally, the two methods should match within a few percent relative error. Unfortunately, we discover large discrepancies between the two methods. If the WAT limit is of interest, the engineer should really solve the general solution equation of motion.

A. Basic Trades – Second Segment (CONF 2)

Figure 6 shows the relationship between the required second segment climb (*V2*) speeds in indicated (equivalent) airspeed as a function of the weight of our notional A320. As expected, the *V2* speed increases as a function of aircraft weight. This is because the *V2* speed is 1.13 times the stall speed, which is a direct function of the weight of the aircraft. Minimum control airspeed on the A320 is low enough that it does not impact the *V2* speed schedule at any of our proposed analysis weights.

This trend leads to a direct correlation between the dimensional drag of the aircraft and the weight of the aircraft. As the airspeed increases, the dynamic pressure increases which, in turn, increases the dimensional skin friction drag. As weight increases, the induced drag also increases. Thus, the total drag increases from the combined effects of skin friction and induced drag. This relationship between drag and weight are plotted in Figure 7. Since we need excess thrust (*T-D > 0*) for a positive climb gradient, the thrust as a function of aircraft weight is plotted alongside the drag.

Figure 7 highlights a worrisome combination of thrust and drag that leads to worsened climb gradient with increasing aircraft weight. As we increase aircraft weight, the dimensional drag increases while our total available thrust *decreases* due to ram drag effects on the engines. From our work-energy theorem, we hold that climb gradient is proportional to *(T-D)/W*. As we increase our takeoff weight, we are simeultaneously decreasing thrust and disproportionately increasing drag. The numerator gets smaller, while the denominator gets larger. This results in a marked degredation of our climb gradient.

We demonstrate this trend in Figure 8. Here we show how climb gradient degrades from ~8.2% at 120,000-lbm to less than 2% at 175,000-lbm. The erosion of the climb gradient with increasing weight creates the dilemma where maximum payload (corresponding to maximum profit from an operational standpoint) is

often located right at the edge of the "legal takeoff point. Hence, airlines are incentivized to push their aircraft to their maximum takeoff capability, which in turn correlates to the point with the lowest margin of safety. Multiple regulatory safeguards are in place to prevent this margin of safety from becoming critically low. For example 14 CFR § 25.121 limits dispatch to circumstances where the 2nd segment climb gradient exceeds 2.4% for two-engined aircraft (this is the formal WAT limit). [13] Regulation 14 CFR § 25.115 requires dispatch to include an additional 0.8% climb gradient safety "buffer" for obstacle clearance planning. [14]

Since we are incentivized to take the point with the lowest margin of safety, we must expand our trade space by realizing that the climb gradient is not a simple function of weight. As the climb gradient relies on the thrust of the engines and the potential lift of the aircraft, it is thus affected by atmospheric conditions. Deviation in temperature and air density (such as at different altitudes) can create stark differences in the WAT limit of the aircraft. The effect on thrust alone is significant, as Figure 9 demonstrates.

From Figure 9, we can see that there is a very significant reduction in thrust with increasing temperature. Engines are typically governed or "flat-rated" to provide thrust relatively insensitive to temperature below certain limiting conditions. Above this, basic thermodynamic considerations, particularly the maximum turbine inlet temperature, begin to affect thrust. The warmer the inlet air, the less fuel can be added before the combustion temperature exceeds this limit. Thus, above the "flat-rate," positive temperature deviations result in far less thrust than at standard temperature conditions; for this NPSS model of the *V*2527 we see that a 5°C deviation can result in a thrust degredation of nearly 1,000-lbf per engine. Increasing altitude also results in a reduction in thrust, although in a less powerful manner. As we rise in altitude, the air density decreases reducing the mass flow through the engine reducing overall thrust.

The effect of the thrust lapse is extremely evident in the WAT limit chart; see Figure 10. A very sharp cliff is formed at positive temperature deviations above the "flat-rate." We see that small deviations in temperature and altitude can create marked changes in the WAT limit of the aircraft that may not be directly visible from standard methods for computing maximum takeoff weight.

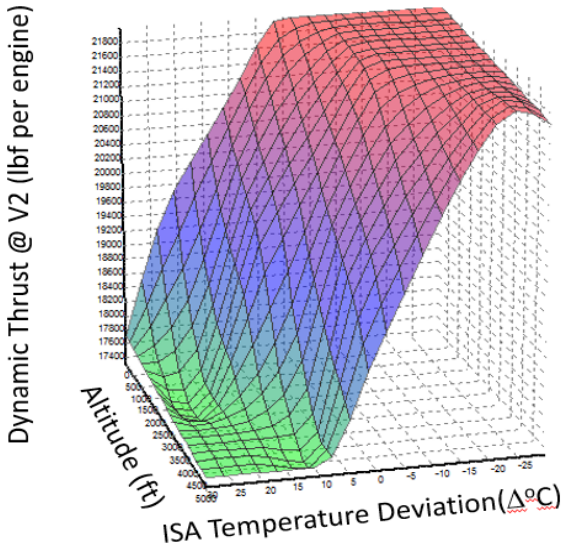

FIGURE 9: Altitude and Temperature Effects on Thrust at *V2* speeds. Aircraft TOW at 175000-lbm Full Takeoff Power. Notional IAE *V*2527-A6 engine (flat rate below sea-level / standard day – might not be quite representative of the real engine).

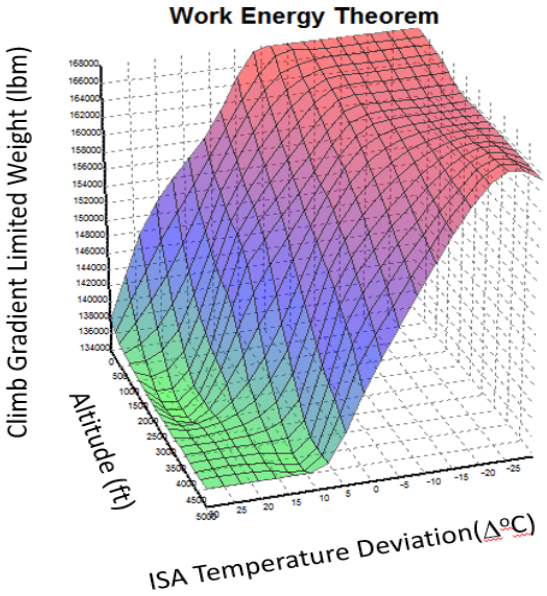

FIGURE 10: 2.4% climb gradient (as calculated by work-energy theorem) limited weight as a function of Altitude and Temperature. Notional A320 model with CONF 2 flap setting, *CLmax* = 2.16, *V2*=1.13 Vs not limited by *VMCA*) with notional IAE *V*2527-A6 engine (flat rate below sea-level / standard day – might not be quite representative of the real engine).

For example, a deviation from standard to +5ºC to +10ºC at sea level results in a change of WAT limited dispatch weight from 165,000-lbm through 161,000-lbm to 158,000-lbm. A 3,000-lbm difference accounts for nearly 12 passengers and their bags, creating a non-insignificant cost incentive for airlines to use the more optimistic estimation. This establishes a dangerous path where airlines may be pushed to rely heavily on the 14 CFR § 25.115 safety margins by disregarding temperature increases during takeoff. It is not unreasonable to see a temperature deviation of +5ºC along the takeoff route, which could have serious impacts on the climb performance of the aircraft.

B. More Complex Trades – full equations of motion (including Const KIAS climb correction)

It becomes increasingly important to have as accurate estimations of our climb gradient as possible in order to better understand the dispatch dillemma formed by the WAT-limit cliff. From solving the full non-linear equations of motion, we can get a more accurate understanding of the takeoff limits of the aircraft. For the studies performed in this section, the full equations of motion were solved from the A320 aerodynamic model developed for **CONF 2** flap deployment.

The results of a takeoff weight trade at sea-level, standard atmosphere conditions can be seen in Figure 11. Here we compare the simple work energy gradient to the exact gradient for unaccelerated flight and the exact gradient computed for climb at constant IAS.

From this graph, we can immediately see that the work energy method appears to be slightly pessimistic (or "conservative") in its estimations, providing a worse climb gradient than the full exact solution at all takeoff weights shown. However, the exact solution and the work energy gradient are very similar, making it hard to determine the full nuance.

To get a better understanding of their relationships, we can zoom-in on the heavy-weight side as most aircraft will be dispatched at higher takeoff weights. The heavy-weight trade can be seen in Figure 12.

Some grittiness is revealed here because we are scheduling *V2* speeds to the nearest integer

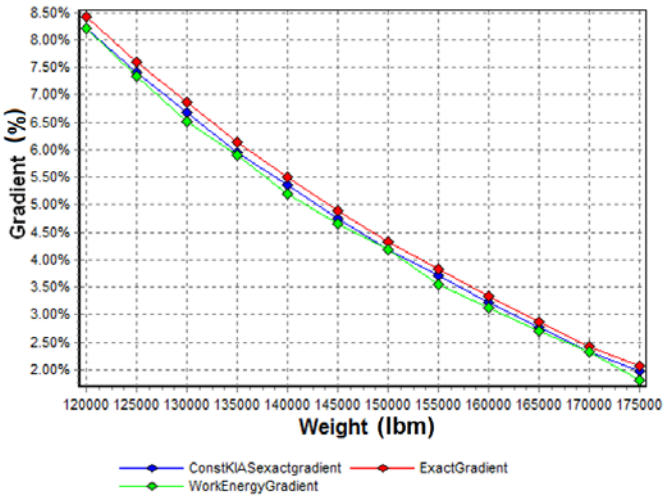

FIGURE 11: climb gradient as a function of takeoff weight comparing the simplified gradient equation (thrust minus drag over weight) with the full equations of motion for unaccelerated climb, and the full equations of motions with a constant IAS climb correction. Notional A320 model with CONF 2 flap setting, *CLmax* = 2.16, *V2*=1.13 *Vs* not limited by *VMCA* powered by notional IAE *V*2527-A6 engine (flat rate below sea-level / standard day – might not be quite representative of the real engine. Simulation ran at standard day sea-level conditions.

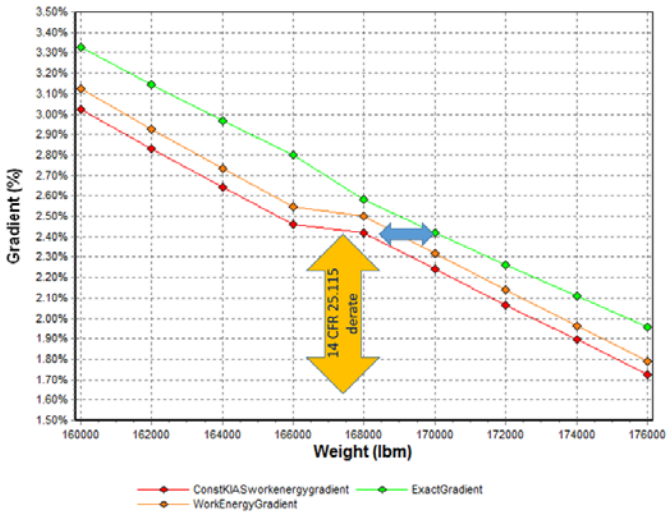

FIGURE 12: zooming in on the high weight corner of the climb gradient as a function of takeoff weight comparing the simplified gradient equation (thrust minus drag over weight) with the full equations of motion for unaccelerated climb, and the full equations of motions with a constant KIAS climb correction applied to this. Notional A320 model with CONF 2 flap setting, *CLmax* = 2.16, *V2*=1.13 *Vs* not limited by *VMCA*) with notional IAE *V*2527-A6 engine (flat rate below sea-level / standard day – might not be quite representative of the real engine). Simulation ran at standard day sea-level conditions.

KIAS (i.e. 170-KIAS vs 171-KIAS rather than 170.34659-KIAS). This was done to better simulate real-world takeoff conditions, as most pilot handbooks list *V2* speeds to the nearest KIAS.

Despite the grittiness, we can readily see that there is a nearly 2,000-lbm discrepancy between the exact gradient and the work-energy gradient in Figure 12. From this perspective, a positive can be found in calculating the exact gradient for aircraft dispatch: airlines can fit 2,000-lbm more cargo on the aircraft while still ensuring FAA climb gradient requirements if their dispatch codes calculate the exact gradient as opposed to using the simple *(T-D)/W* work-energy gradient. 2,000-lbm corresponds to nearly eight extra passengers and respective baggage, providing a cost incentive to calculate the exact gradient.

Another perspective that can be used in viewing this data is in the climb-gradient discrepancy. The exact gradient has an ~0.2% discrepancy agsint the work-energy gradient. In comparison, 14 CFR § 25.115 requires a 0.8% extra gradient capability. The discrepancy created by the difference in method is only 25% the discrepancy built-in by federal regulations, providing more reason to apply the exact gradient as any discrepancy is almost assuredly absorbed by the 14 CFR § 25.115 derate. [14]

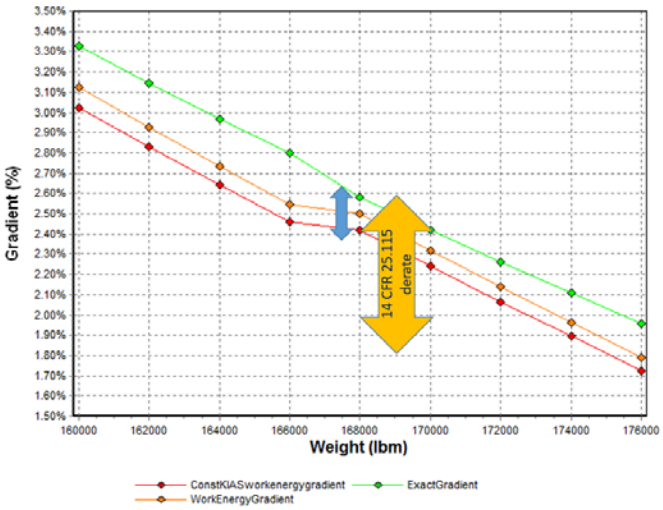

FIGURE 13: zooming in on the high weight corner of the climb gradient as a function of takeoff weight compariing the simplified gradient equation (thrust minus drag over weight) with the full equations of motion for unaccelerated climb, and the full equations of motions with a constant KIAS climb correction applied to this. Notional A320 model with CONF 2 flap setting, *CLmax* = 2.16, *V2*=1.13 *Vs* not limited by *VMCA*) with notional IAE *V2*527-A6 engine (flat rate below sea-level / standard day – might not be quite representative of the real engine). Simulation ran at standard day sea-level conditions.

This brings up a crucial point: although we appear to have a non-insignificant gain in WAT-limited takeoff-weight when compared to the work-energy gradient, the code of federal regulations nor the FAA require airlines or aircraft designers to specify *which* climb gradient estimation they are using. If either party uses a more optimistic method than the exact gradient, the benefits seen from using the gradient over the work-energy theorem will be inverted. Although the 0.8% federal derate helps reduce discrepancies, an overly-optimistic gradient calculation would potentially create a flight-into-terrain hazard when dispatching an aircraft on the "WAT limit cliff" (return to Figure 10). This begs the question as to whether the added risk from optimistic approaches is worth the benefit. We believe that the best way to maximize profits and safety is to simply use an exact climb gradient calculation with constant IAS corrections. This ensures that the aircraft is capable of meeting all takeoff requirements, while firmly grounding its takeoff capabilities in reality via the full equations of motion.

From Figure 12 and 13, we can see that although there is not a large difference between the methods in terms of the gradient magnitude, there is a more significant boost in allowable takeoff weight from the exact climb gradient compared to the work-energy theorem. However, these results are only valid for standard-day conditions, and as we have seen with Figure 11 and 12 there is a large variance in the climb-gradient weight limit due to non-standard day conditions.

The effects of temperature and altitude devation for the exact climb-gradient WAT limit are thus plotted in Figure 14, overleaf. In this surface plot, we see that the general trends for WAT limits between the work-energy theorem and the exact climb-gradient are extremely similar. However, one can see that there is a slightly flatter plateau at the low

altitude, low temperature location, which could potentially result in beneficial weight differences. The maximum exact climb gradient weight limit is also slightly higher than than the work-energy theorem WAT limit, as the exact climb gradient reaches weights of ~169,000-170,000-lbm while the work-energy theorem WAT limit was weight-limited to ~168,000-lbm.

To more clearly see the differences between the work-energy theorem wat limit and the exact climb gradient, the difference in WAT-limit weight from the exact gradient to work-energy gradient is plotted as a function of altitude and temperature deviation; turn to Figure 15. It is immediately clear that the difference between these two methods is highly nonlinear and "gritty." Curiously, we can see a maximum difference occur at an altitude of about 2000-ft, where the exact climb-gradient WAT limit allows for ~3,000-lbm extra dispatch weight than the work-energy climb gradient. However, at low and high altitude variations the difference between the methods is much smaller at only ~1,000-lbm. The temperature deviation also shows an interesting shape, where there is a steeper difference at altitude than at sea-level.

V. Recommendations and Conclusions

This work shows that the predicted performance arising from the full equations of motion differs from that predicted by a simplified, work-energy-theorem model. If WAT limits are of interest, the engineer should solve the general solution equation of motion. This is at odds with the Boeing Performance Short Course [28] and most other textbooks. [24][25][26][27]

Solutions of the full equations of motion demonstrate that the climb performance of an aircraft is primarily influenced by its thrust-to-weight and its aerodynamic efficiency. These trends are fully captured by the *(T-D)/W* formula, even if this equation is an inexact approximation of reality. What the *(T-D)/W* misses are the relationships that are obscured by the unusual "small-angle-approximation" used in the classical derivation: that $\sin(\alpha+\gamma) = 0$; $\cos(\alpha+\gamma) = 1$. The choice of climb speed, the zero-lift-drag, wing sweep and wing aspect ratio all impact the lift-curve-slope and the drag reduction that arises as terms proportional to $\sin(\alpha+\gamma)$ grow in magnitude.

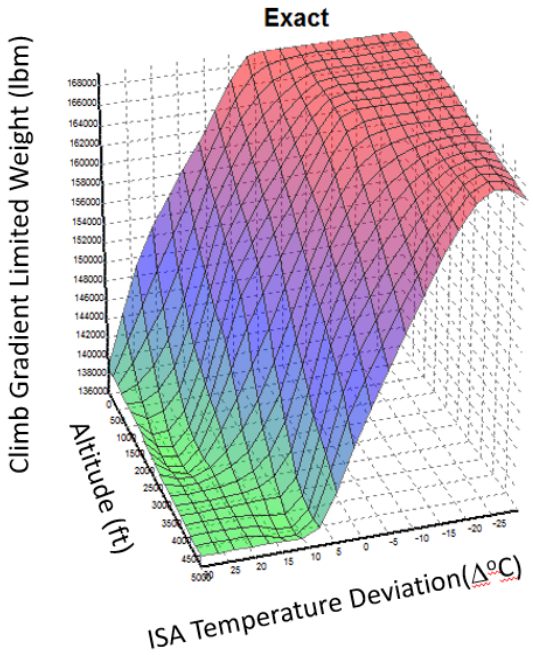

FIGURE 14: 2.4% climb gradient (as calculated by exact angle solution) limited weight as a function of Altitude and Temperature. (notional A320 model with CONF 2 flap setting, *CLmax* = 2.16, Vs=1.13 Vstall not limited by *VMCA*) with notional IAE *V*2527-A6 engine (flat rate below sea-level / standard day – might not be quite representative of the real engine).

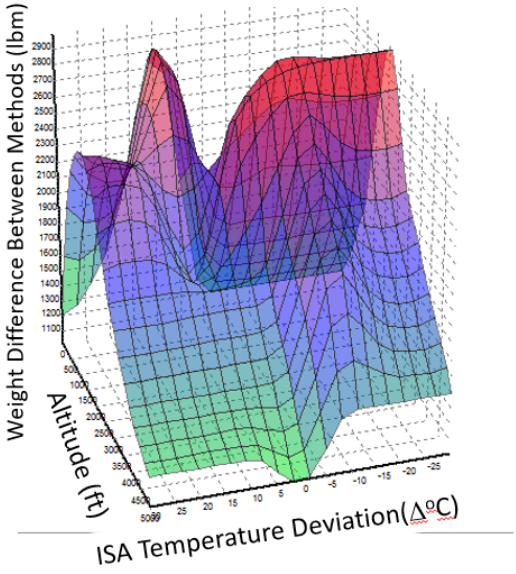

FIGURE 15: Delta between exact climb-gradient WAT limit (Figure 14) and work-energy WAT limit (Figure 10).

An important takeaway from Figure 15 is that the exact climb gradient allows for more weight than the work-energy theorem throughout a wide range of altitudes and temperatures. This means that the work-energy theorem appears to be a wholly conservative estimate even throughout temperature and altitude variations. Hence, from an airline operations standpoint, there may be significant monetary benefit from calculating the exact climb-gradient of an aircraft vs using the work-energy approximation as the exact gradient provides for at least 1000-lbm extra cargo (about 4 passengers). There is also minimal safety loss by calculating via the exact climb-gradient method, as the difference in weight is minimal as compared to the 14 CFR § 25.115 safety buffer. [14]

Although there are potentially numerous other methods for estimating the climb gradient, it is our recommendation that the exact climb-gradient calculation is used for operational purposes. Considering the large and somewhat chaotic perturbations found in the difference between the work-energy theorem and the exact method (Figure 15), it is very likely that other estimation techniques will result in highly nonlinear differences as well. The exact method is a purely physics-based approach that is valid at all takeoff conditions, and by its nature does not use any simplifications and thus does not have any implicit constraints. This makes the exact method highly useful for dispatch planning purposes as it is guaranteed to properly model the aircraft's takeoff without unknown variances.

If safety is of concern, it is still recommended to calculate the exact climb-gradient rather than the work-energy theorem, as the difference from the work-energy theorem is highly non-linear and thus the actual safety margin for a particular weight, altitude, and temperature deviation is unknown. Calculating the exact-climb gradient and applying a constant safety factor provides a more consistent approach that ensures a proper safety overhead at all takeoff conditions.

Acknowledgments

Prof. Takahashi wants to give special thanks for Phoenix Integration for supplying Arizona State with *ModelCenter*.

References

1. Wood, D.L. and Takahashi, T.T., "Extraordinary Care: A History of Flight Operations Rules for Common Carriers," AIAA 2018-1616, 2018
2. *See* 14 CFR § 25 generally
3. *See* 14 CFR § 91 generally
4. *See* 14 CFR § 121 generally
5. 14 CFR § 25.105 (2018) "Takeoff"
6. 14 CFR § 25.109 (2018) "Accelerate-Stop Distance"
7. 14 CFR § 25.113 (2018) "Takeoff Distance and Takeoff Run"
8. 14 CFR § 121.189 (2018) "Airplanes: Turbine Engine Powered – Takeoff Limitations"
9. 14 CFR § 121.191 (2018) "Airplanes: Turbine engine powered: En route limitations: One engine inoperative."
10. Delisle, M. and Takahashi, T.T., "Speed Stability and Obstacle Clearance During Engine Inoperative Takeoff," AIAA 2018-3502, 2018.
11. Beard, J.E. and Takahashi, T.T., "(Un)controlled Flight Into Terrain: A History of Obstacle Clearance Regulations," AIAA 2018-1614, 2018.
12. Beard, J.E. and Takahashi, T.T., "Optimal Piloting Approaches For Obstacle Clearance Limited Standard Instrument Departures," AIAA 2018-0285, 2018.
13. 14 CFR § 25.121 (2018) "Climb: One Engine Inoperative"
14. 14 CFR § 25.115 (2018) "Takeoff Flight Path"
15. 14 CFR § 25.111 (2018) "Takeoff Path"
16. 14 CFR § 25.904 (2018) "Automatic Takeoff Thrust Control System"
17. 14 CFR § 25 APPENDIX I
18. 14 CFR § 25.107 (2018) "Takeoff Speeds"
19. 14 CFR §25.123 (2018) "En Route Flight Paths"
20. EASA CS 25.107
21. EASA CS 25.111

22. EASA CS 25.121
23. *See* https://en.wikipedia.org/wiki/Newton%27s_laws_of_motion (retrieved March 5, 2018)
24. Anderson, J.D., *Aircraft Performance and Design*, McGraw-Hill, New York, 1999.
25. Roskam, J. and Lam, C., *Airplane Aerodynamics and Performance*, DAR Corporation, Lawrence, KS, 1997.
26. Raymer, D.P., *Aircraft Design: A Conceptual Approach*, AIAA, Washington DC, 1989.
27. Nicolai, L.M., *Fundamentals of Aircraft Design*, METS, San Jose, CA, 1984.
28. Anon., *Jet Transport Performance Methods*, Boeing Flight Operations Engineering Training Document D6-1420, 7th Edition, Boeing, Seattle, WA, May 1989.
29. Takahashi, T.T., *Aircraft Peformance & Sizing*, Vol I & II, Momentum Press, New York, 2018.
30. Takahashi, T.T., "Optimal Climb Trajectories Through Explicit Simulation," AIAA 2015-2701, 2015.
31. Takahashi, T.T., Beard, J.E. and Wood, D.L., "The Human Factor: Accounting For "Off Book" Flight Speeds Within Implied Safety Margins," AIAA 2018-0284, 2018.
32. Takahashi, T.T., "A Bad Moon Rising: The Puzzling Inaccuracies of the Work-Energy Theorem in Aircraft Performance," AIAA 2019-1305, 2019.
33. Airbus Industrie A320 Model A320-212 Flight Manual. (1990). Blagnac, France: approved by D.G.A.C.
34. Beard, J.E. "Takeoff Obstacle Clearance Procedures: The Feasibility of Extended Second Segment Climb " M.S. Thesis, Arizona State University, April 2017.
35. Numerical Propulsion System Simulation Consortium, NPSS User's Guide, Numerical Propulsion System Simulation Consortium, 2016.
36. See https://en.wikipedia.org/wiki/IAE_V2500 (retrieved April 23, 2019)